Supporting Information

for

Shape Effect of Glyco-nanoparticles on Macrophage Cellular Uptake and Immune Response

Zhen Li,[#1] Liang Sun,[#2] Yufei Zhang,[1] Andrew P. Dove,[2] Rachel K. O'Reilly*[2] and Guosong Chen*[1]

[#]These authors contributed equally.

[1]The State Key Laboratory of Molecular Engineering of Polymers and Department of Macromolecular Science, Fudan University, Shanghai, 200433 China

[2]Department of Chemistry, University of Warwick, Coventry CV4 7AL, U.K.

Materials

Chemicals and solvents were used as purchased from Aldrich, Acros, Fluka, Fisher Chemical, Alfa Aesar, VWR or J&K Chemical. *L*-Lactide and *DL*-lactide monomers were kindly donated by Corbion-Purac and were passed through a silica plug with dichloromethane (CH_2Cl_2) as eluent to remove impurities and then dried over 3Å molecular sieves in CH_2Cl_2. *L*-Lactide monomer was

further purified by recrystallization in toluene before being stored in a glove box under an inert atmosphere. (-)-Sparteine was dried CaH_2 before use and 1-(3,5-bis(trifluoromethyl)phenyl)-3-cyclohexyl-thiourea was prepared and purified as previously reported.[1] Tetrahydropyran acrylate (THPA) was synthesized and purified as described previously.[2, 3] 2,2-Azobis(isobutyronitrile) (AIBN) was recrystallized from methanol and stored at 4 °C. Dichloromethane (CH_2Cl_2), *N*,*N*-dimethylformamide (DMF) were purified using a solvent purification system (PS-MD-3, Innovative Technology Inc., USA) before use. Unless specially mentioned, all other chemicals were used as received.

Instrumentations

NMR

^{1}H nuclear magnetic resonance (^{1}H NMR) spectra and ^{13}C nuclear magnetic resonance (^{13}C NMR) were recorded on a Bruker DPX-400 spectrometer. The chemical shifts are given in ppm with tetramethylsilane (TMS) as an internal reference.

SEC

Size exclusion chromatography (SEC) was performed on an 1260 Infinity Multi-Detector SEC instrument equipped with

differential refractive index with $CHCl_3$ and 0.5% triethylamine as eluent at a flow rate of 1 mL/min. SEC data was analyzed using Cirrus GPC software with PS standards used for calibration.

MALDI-TOF MS

The matrix-assisted laser desorption ionization time-of-flight mass spectrometry (MALDI-TOF MS) measurement was performed using AB SCIEXMALDI-TOF/TOF MS 5800 System, using THAP as matrix in reflection mode.

Zeta potential

The zeta potentials of the nanoparticles were determined with a Zetasizer Nano-ZS from Malvern Instruments.

TEM

Transmission electron microscopy (TEM) images were taken with a Tecnai G2 instrument operating at an accelerating voltage of 200 TEM samples were prepared as follows: Generally, formvar/carbon grids were cleaned by air plasma from a glow-discharge system before use, which also improved the hydrophilicity character of the grids. Then one drop of the sample solution (0.25 mg/mL, 20 μL) was deposited on a carbon grid and after 2 min, the solution was blotted away before drying totally in the air. For the stained sample, 5 μL of 2 wt% neutralized phosphotungstic acid (PTA) solution was then added on the grid to stain the particles and was blotted away

after 30 s before air drying. TEM images were analyzed by ImageJ software, and 150 particles (the stained samples) were counted for each sample to obtain the number-average length (L_n) and to calculate weight-average length (L_w), number-average width (W_n) (for cylindrical micelles) and number-average diameter (D_n) (for spherical micelles). L_n, L_w, W_n and D_n were calculated by using the following equations:

$$L_n = \frac{\sum_{i=1}^{n} N_i L_i}{\sum_{i=1}^{n} N_i} \quad (1)$$

$$L_w = \frac{\sum_{i=1}^{n} N_i L_i^2}{\sum_{i=1}^{n} N_i L_i} \quad (2)$$

$$W_n = \frac{\sum_{i=1}^{n} N_i W_i}{\sum_{i=1}^{n} N_i} \quad (3)$$

$$D_n = \frac{\sum_{i=1}^{n} N_i D_i}{\sum_{i=1}^{n} N_i} \quad (4)$$

Where L_i and W_i are the length and the width of each counted cylindrical micelle while D_i is the diameter of each counted spherical micelle. N_i is the number of the cylindrical micelles with the length of L_i and the width of W_i or the number of spherical micelles with the diameter of D_i.

DLS

Dynamic light scattering (DLS) studies were conducted using ALV/5000E laser light scattering (LLS) spectrometers at 90°, CONTIN analysis was used for the extraction of $<R_h>$ data. Prior to characterization, various micelles (0.25 mg/mL in aqueous solution)

were filtered through 0.8 micron filters (MF-Millipore MCE Membrane) to remove dust.

UV-vis

Ultraviolet–vis (UV-vis) absorption spectra were recorded by a Shimadzu UV-2550 spectrophotometer with a 1 mm cuvette.

FLS

The steady-state fluorescence measurements were recorded on a FLS 920 (Edinburg Instruments) spectrofluorophotometer (488 nm excitation).

Flow cytometry

Flow cytometry data were obtained using Gallios (Beckman Coulter) flow cytometer.

CLSM

Confocal laser-scanning microscopy images were taken from Nikon C2+.

Experimental Section

Synthesis of PLLA and PDLLA Using ROP

PLLA and PDLLA were synthesized in a glove box under nitrogen atmosphere by ROP using a dual-headed initiator that was

previously reported.[4, 5] Generally, initiator (83.0 mg, 0.21 mmol), and (-)-sparteine (59.8 µL, 0.26 mmol) were combined in one vial with *L*-lactide (or *DL*-lactide) (1.5 g, 10.4 mmol) and 1-(3,5-bis(trifluoromethyl)phenyl)-3-cyclohexyl-thiourea (192.7 mg, 0.52 mmol) in another. CH_2Cl_2 (2 mL and 4 mL for each vial respectively) was then added to each of the vials before the two solutions were mixed and left to stir at room temperature for 3.5 h. Product was precipitated in *n*-hexane three times before filtration and dried *in vacuo* to yield a yellow solid. ^{1}H NMR (400 MHz, $CDCl_3$, ppm, Figure S1 and Figure S2) δ 7.37 - 7.29 (4H, m, H6 & H7), 5.39 – 4.91 (2H PLA +2H, m, H8 & H9 & H11), 4.61 (2H, s, H5), 3.37 (2H, t, $^3J_{H\text{-}H}$ = 7.5 Hz, H4), 1.75 - 1.40 (6H PLA + 2H, m, H10 & H12 & H3), 1.34 - 1.17 (18H, br, H2), 0.88 (3H, t, $^3J_{H\text{-}H}$ = 6.5 Hz, H1) ; $Đ_M$ of PLLA (SEC, $CHCl_3$ and 0.5% TEA as eluent, Figure S5) = 1.06; $Đ_M$ of PDLLA (SEC, $CHCl_3$ and 0.5% TEA as eluent, RI detection, Figure S6) = 1.05.

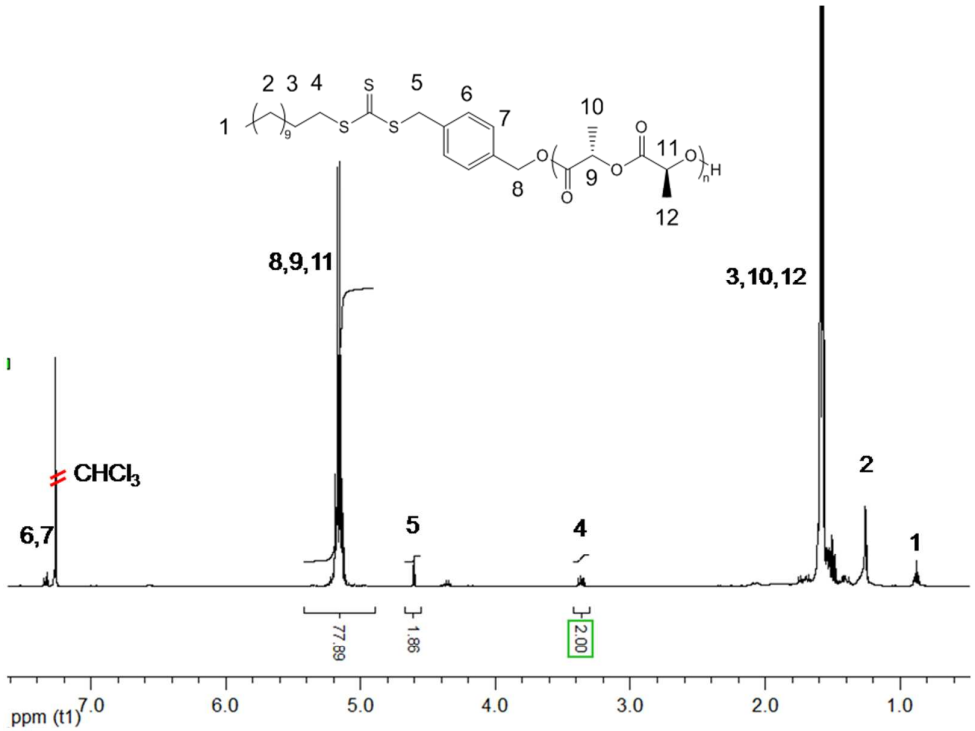

Figure S1. ^{1}H NMR spectrum (400 MHz, $CDCl_3$) of $PLLA_{39}$ macro-initiator.

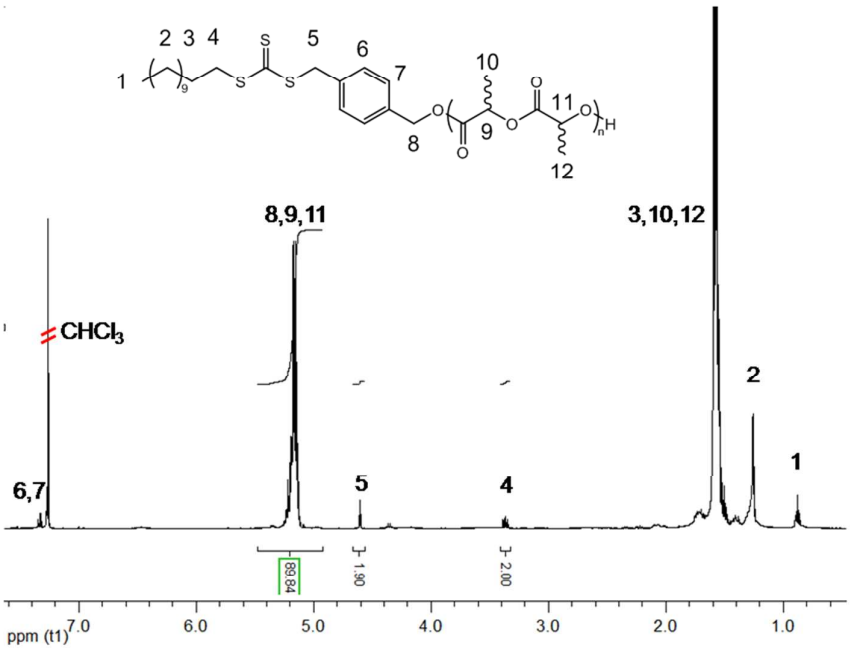

Figure S2. ^{1}H NMR spectrum (400 MHz, $CDCl_3$) of $PDLLA_{45}$ macro-initiator.

Synthesis of PLLA-*b*-PTHPA and PDLLA-*b*-PTHPA Diblock Copolymers Using RAFT Polymerization

Generally, THPA (2.5 g, 0.016 mol) and PLLA macro-initiator (or PDLLA macro-initiator) (0.115 g, 0.020 mmol), were dissolved in $CHCl_3$ (2.5 mL) and transferred into a dried ampoule before adding AIBN (32.9 μL of a 10 mg/mL $CHCl_3$ solution, 0.002 mmol). The solution was degassed by three freeze-pump-thaw cycles and sealed under argon and then placed in a 60 °C oil bath with stirring for 1.8 h. The product was precipitated into *n*-hexane three times and dried *in vacuo* to give a pale yellow solid. ^{1}H NMR (400 MHz, $CDCl_3$, ppm, Figure S3 and Figure S4) δ 6.20 - 5.68 (1H PTHPA, br, H5), 5.25 - 5.04 (2H PLA + 2H, m, H11 & H13 & H10), 4.03 - 3.50 (2H PTHPA, br, H9), 2.54 - 2.20 (1H PTHPA, br, H3), 2.15 - 1.36 (8H PTHPA & 6H PLA, br, H4 & H6 & H7& H8 & H12 & H14); $Đ_M$ of PLLA-*b*-PTHPA (SEC, $CHCl_3$ and 0.5% TEA as eluent, Figure S5) = 1.16; $Đ_M$ of PDLLA-*b*-PTHPA (SEC, $CHCl_3$ and 0.5% TEA as eluent, RI detection, Figure S6) = 1.20.

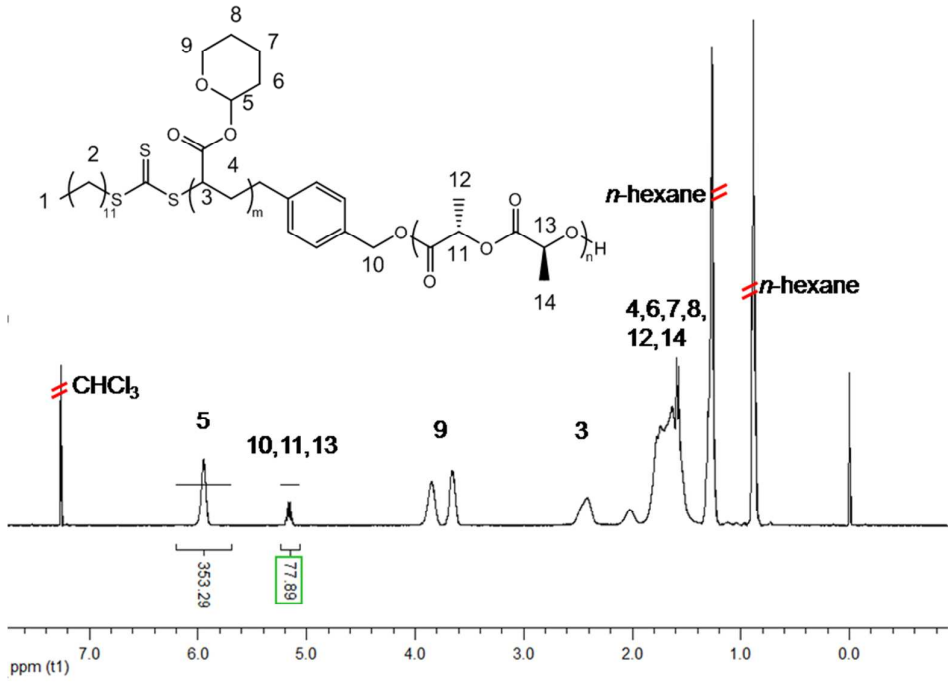

Figure S3. ^{1}H NMR spectrum (400 MHz, $CDCl_3$) of $PLLA_{39}$-*b*-$PTHPA_{353}$.

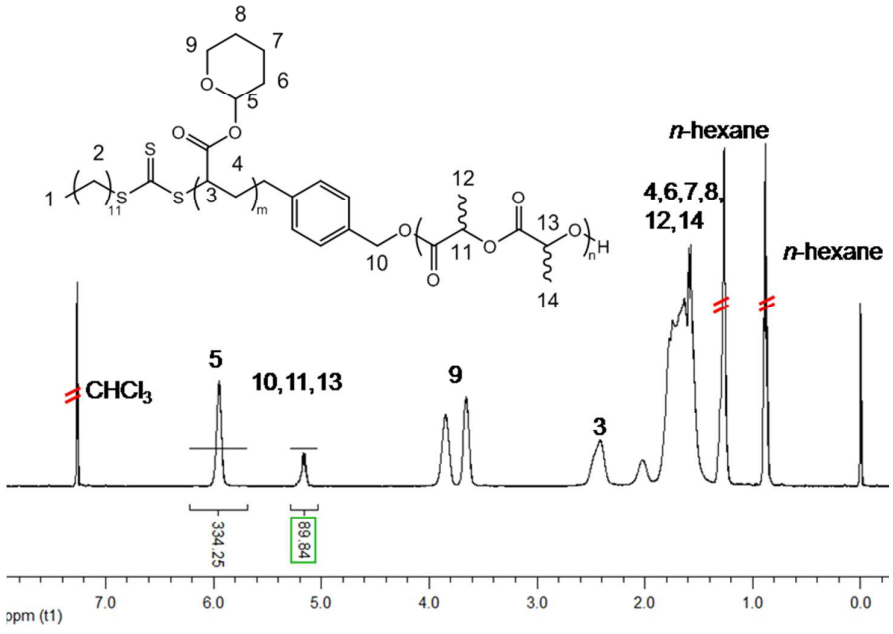

Figure S4. ^{1}H NMR spectrum (400 MHz, $CDCl_3$) of $PDLLA_{45}$-*b*-$PTHPA_{334}$.

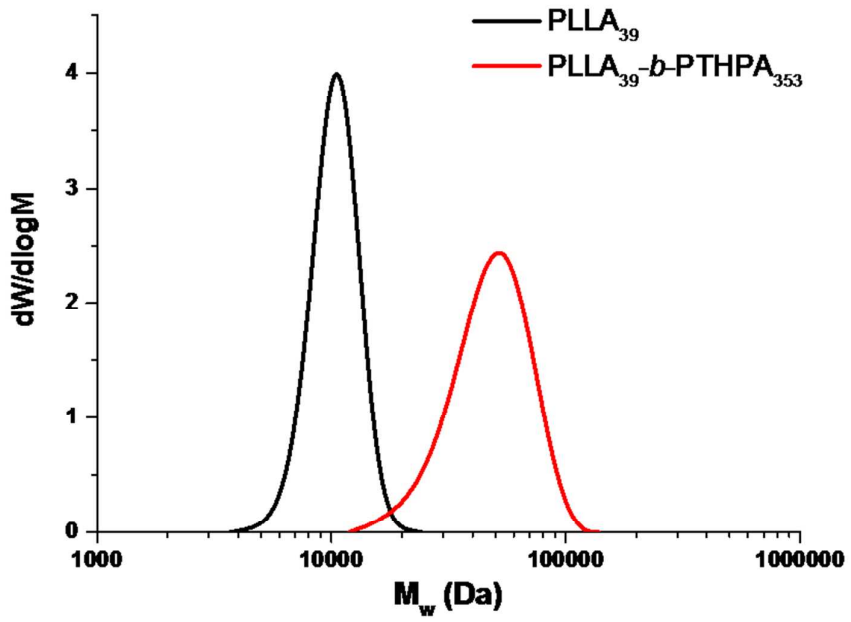

Figure S5. SEC traces ($CHCl_3$ + 0.5% TEA) of $PLLA_{39}$ and $PLLA_{39}$-*b*-$PTHPA_{353}$.

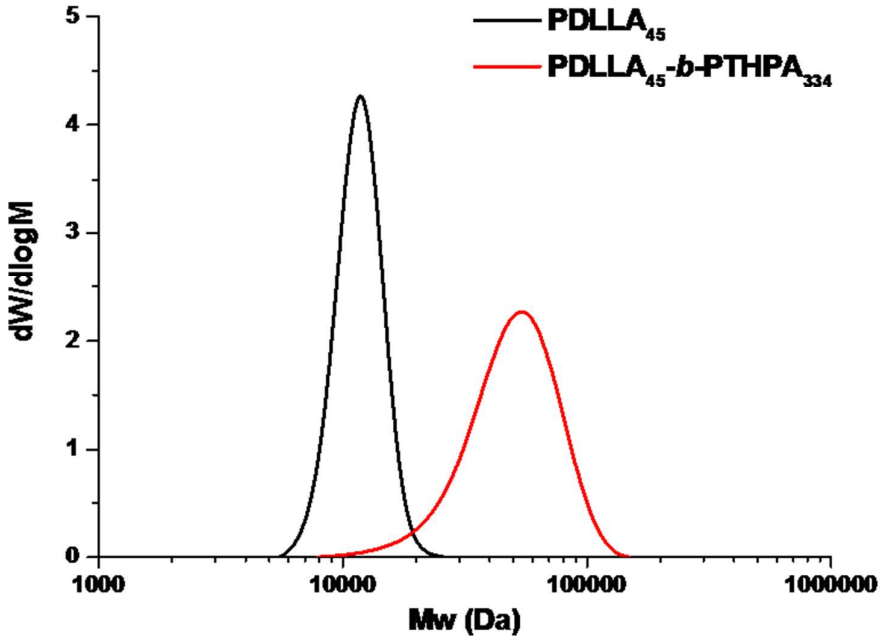

Figure S6. SEC traces ($CHCl_3$ + 0.5% TEA) of $PDLLA_{45}$ and $PDLLA_{45}$-*b*-$PTHPA_{334}$.

Table S1. Characterization data of PLLA-*b*-PTHPA and PDLLA-*b*-PTHPA diblock copolymers

Polymer	M_n[a] (kDa)	$Đ_M$[b]	Hydrophobic wt%[c]
$PLLA_{39}$-*b*-$PTHPA_{353}$	61.2	1.16	18.1
$PDLLA_{45}$-*b*-$PTHPA_{334}$	59.0	1.20	21.2

[a] Measured by ^1H NMR spectroscopy (400 MHz, $CDCl_3$). [b] Measured by SEC analysis ($CHCl_3$ with 0.5% TEA as eluent). [c] PLA weight fraction in the PLA-*b*-PAA diblock copolymer.

Synthesis of 2-(2-(2-azidoethoxy)ethoxy)ethanol

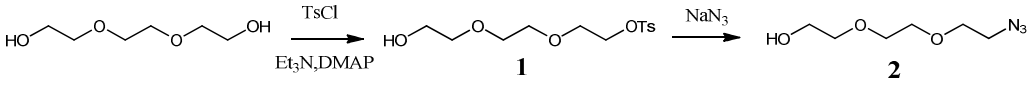

Triethylene glycol (11 g, 73.3 mmol), triethylamine (2.6 mL, 19.1 mmol) and DMAP (45 mg, 0.37 mmol) were mixed in 100 mL dry dichloromethane at 0 °C. Tosyl chloride (3.5 g, 18.1 mmol) in 20 mL dry dichloromethane was slowly added to the mixed solution within 2 h and the mixture was allowed to stir at room temperature overnight. The resulting mixture was washed with 1 M HCL, H_2O and brine. The extract was dried over $MgSO_4$ and the excess solvent was removed *in vacuo* to yield compound **1** as a yellow oil (4.5 g, 80%). The product was directly used for subsequent reaction without any further purifications.

To a solution of compound **1** (4.5 g, 14.8 mmol) in 20 mL DMF was slowly added NaN_3 (1.92g, 29.5 mmol) at room temperature. Then the mixture was allowed to stir at 80 °C overnight. DMF was evaporated and the solid residue was suspended in Et_2O. The solution was filtered through a Celite bed and the filtrate was concentrated *in vacuo*. The crude was purified using silica gel chromatography (v_{EtOAc} : $v_{petroleum\ ether}$ = 3:1) to obtain compound **2** as a yellow oil (2.3 g, 89%). ^1H NMR (400 MHz, $CDCl_3$) δ 3.74 (s, 2H), 3.71 – 3.67 (m, 6H), 3.64 – 3.60 (m, 2H), 3.41 (t, 2H), 2.48 (s,

2H). ^{13}C NMR (101 MHz, $CDCl_3$) δ 72.49, 70.66, 70.40, 70.07, 61.77, 50.65.

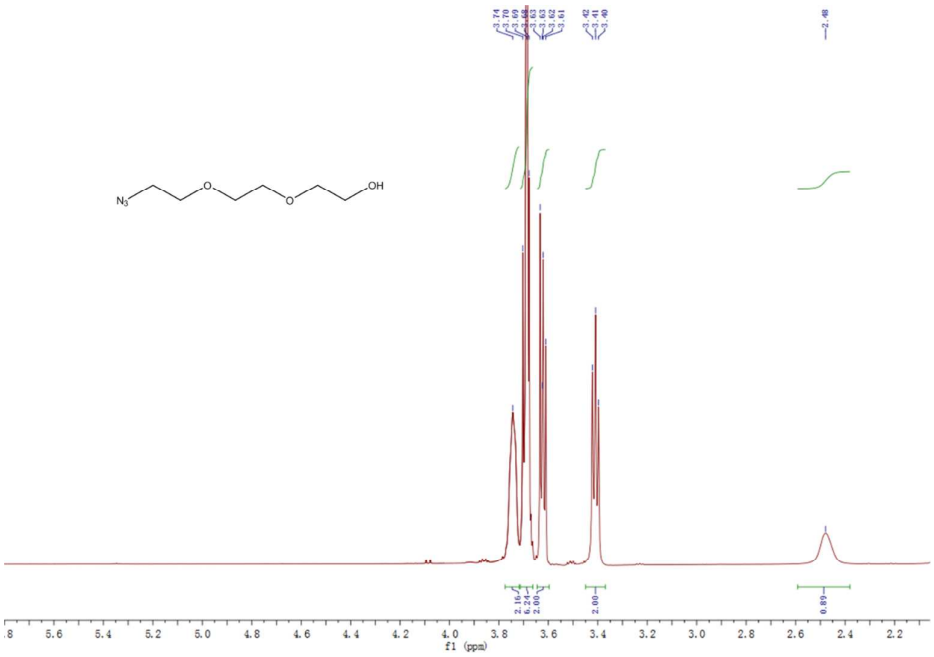

Figure S7. ^{1}H NMR spectrum (400 MHz, $CDCl_3$) of 2-(2-(2-azidoethoxy)ethoxy)ethanol.

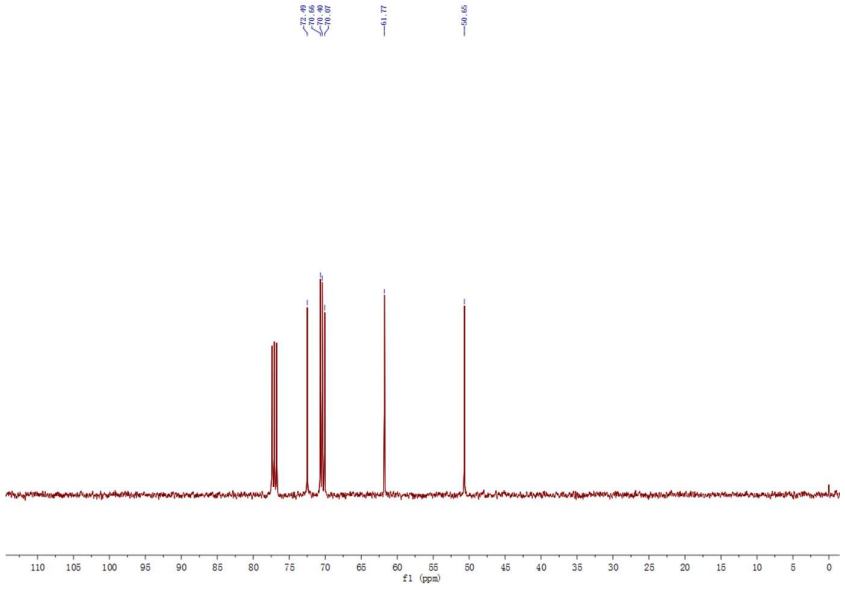

Figure S8. ^{13}C NMR spectrum (101 MHz, $CDCl_3$) of 2-(2-(2-azidoethoxy)ethoxy)ethanol.

Synthesis of 1-(2-(2-(2-Aminoethoxy)ethoxy)ethoxy-D-mannose

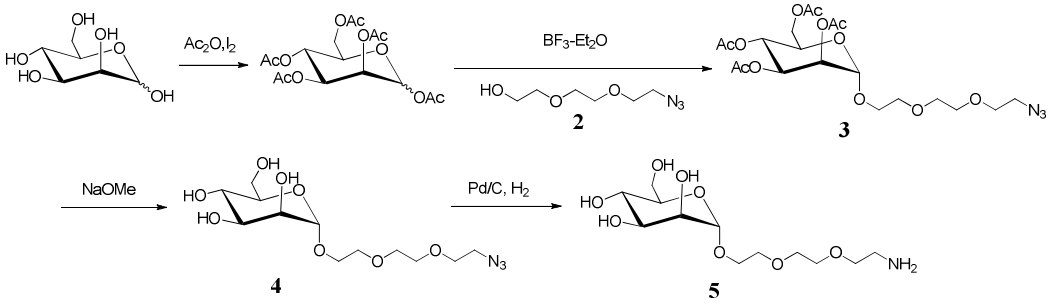

Iodine (0.2 g) was added to a stirred mixture of acetic anhydride (30 mL) and D-mannopyranoside (5.0 g, 27.8 mmol). The reaction mixture was allowed to stir at room temperature until the solid was completely dissolved. The mixture was then diluted with dichloromethane (100 mL) and was washed against saturated Na_2SO_3 aqueous solution, saturated $NaHCO_3$ aqueous solution, brine and water. The extract was dried over $MgSO_4$ and the solvent was evaporated under reduced pressure to yield the pentaacetate (9.74 g) as a pale yellow oil.

A solution of penta-O-acetate-D-mannose (6.0 g, 15.4mmol) and compound **2** (3.3 g, 18.5 mmol) in dry dichloromethane (120 mL) was cooled to 0 °C. The solution was degassed by bubbling nitrogen for 30 minutes, then boron trifluoride diethyl etherate ($BF_3{\cdot}Et_2O$) (10.9 g, 77 mmol) was added dropwise. The mixture was allowed to stir at 0 °C for another 30 min, then at ambient

temperature overnight. The solution was added into ice water, extracted with dichloromethane, and the extract was washed with saturated $NaHCO_3$, brine and dried over $MgSO_4$. The crude product was purified using silica gel column chromatography (v_{EtOAc} : $v_{petroleum\ ether}$ = 1:1), yielding compound **3** (3.83 g, 48%) as a colorless oil. ^{1}H NMR (400 MHz, $CDCl_3$) δ 5.36 (dd, J = 10.1, 3.3 Hz, 1H), 5.30 (d, J = 9.9 Hz, 1H), 5.27 (dd, J = 3.4, 1.8 Hz, 1H), 4.88 (d, J = 1.5 Hz, 1H), 4.29 (dd, J = 12.4, 5.2 Hz, 1H), 4.13 – 4.05 (m, 2H), 3.87 – 3.78 (m, 1H), 3.72 – 3.65 (m, 9H), 3.40 (t, 2H), 2.16 (s, 3H), 2.10 (s, 3H), 2.05 (s, 3H), 1.99 (s, 3H). ^{13}C NMR (101 MHz, $CDCl_3$) δ 170.56, 169.93, 169.79, 169.64, 97.63, 70.72, 70.61, 70.03, 70.00, 69.49, 69.01, 68.34, 67.32, 66.08, 62.35, 50.59, 20.81, 20.67, 20.61.

Compound **3** (3.83 g, 7.58 mmol) was dissolved in methanol (30 mL), and sodium methoxide (3 M in methanol, 5 drops) was added. The reaction mixture was allowed to stir at room temperature for 1 h. Dowex 50WX2 H^+ resin was added to adjust the pH to 7. The mixture was then filtered through Celite and the solvent was evaporated to yield compound **4** (2.50 g, 98%) as a colorless oil. ^{1}H NMR (400 MHz, D_2O): δ 4.87 (d, J = 1.6 Hz, 1H), 3.95 (dd, J = 3.4 Hz, 1.7 Hz, 1H), 3.90 – 3.84 (m, 2H), 3.83 – 3.79 (m, 1H), 3.77 – 3.70 (m, 10H), 3.69 – 3.62 (m, 3H), 3.51 – 3.47 (m, 2H). ^{13}C NMR

(101 MHz, D_2O) δ 99.91, 72.69, 70.46, 69.92, 69.60, 69.51, 69.47, 69.24, 66.69, 66.36, 60.88, 50.11.

Compound **4** (980 mg, 2.9 mmol) was dissolved in methanol (20 mL), and Pd/C (200 mg) was added. The solution was purged with H_2. The mixture was stirred vigorously at room temperature and the complete consumption of the starting material was proven using thin-layer chromatography. The reaction mixture was then filtered through Celite and the solvent was evaporated to yield compound **5** (810 mg, 89%) as a clear oil. Compound **5** was stored under N_2 atmosphere at -20 °C before use. ^{1}H NMR (400 MHz, D_2O) δ 4.79 (d, J = 1.6 Hz, 1H), 3.86 (dd, J = 3.3 Hz, 1.7 Hz, 1H), 3.81 – 3.45 (m, 15H), 2.71 (t, J = 5.4 Hz, 2H). ^{13}C NMR (101 MHz, D_2O) δ 99.91, 72.69, 70.46, 69.92, 69.60, 69.51, 69.47, 69.24, 66.69, 66.36, 60.88, 50.11.MALDI-TOF MS: $[M+Na]^+$ calculated: 334.15; found: 334.14.

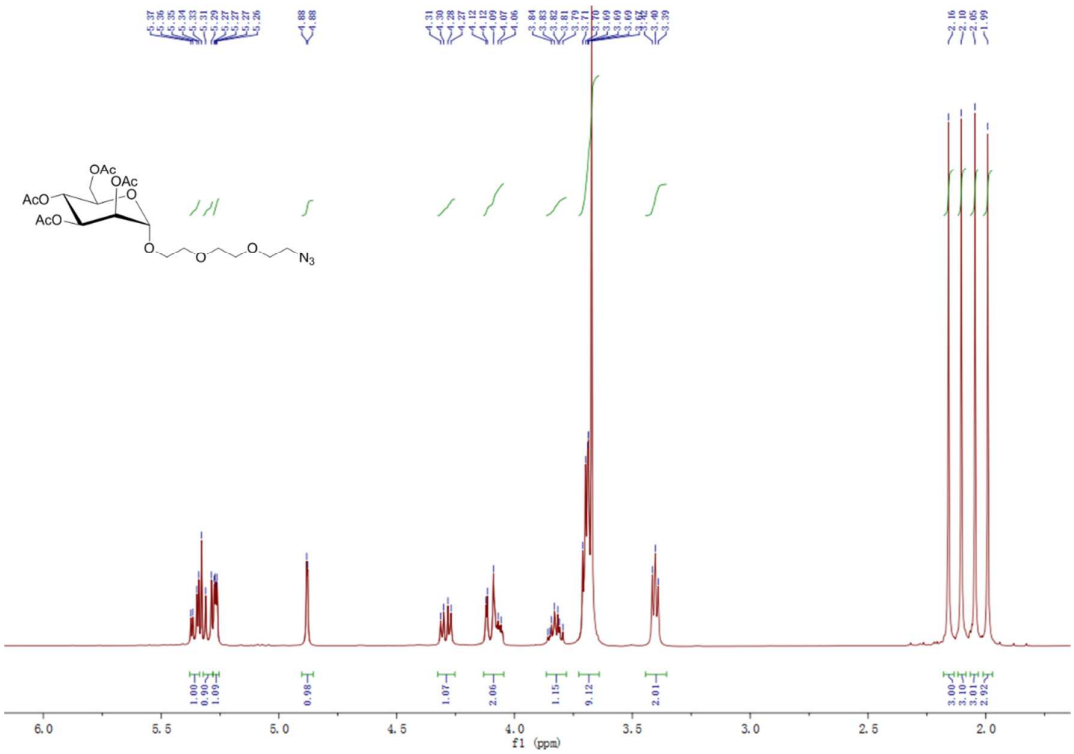

Figure S9. ^{1}H NMR spectrum (400 MHz, $CDCl_3$) of compound **3**.

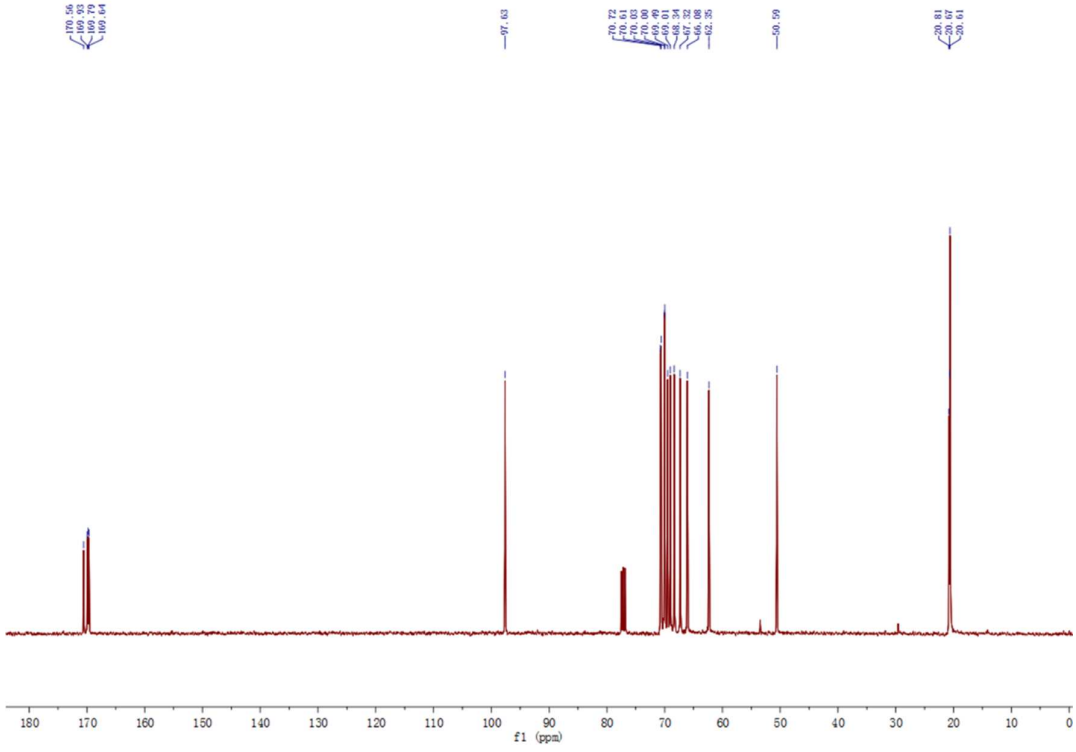

Figure S10. ^{13}C NMR spectrum (101 MHz, $CDCl_3$) of compound **3**.

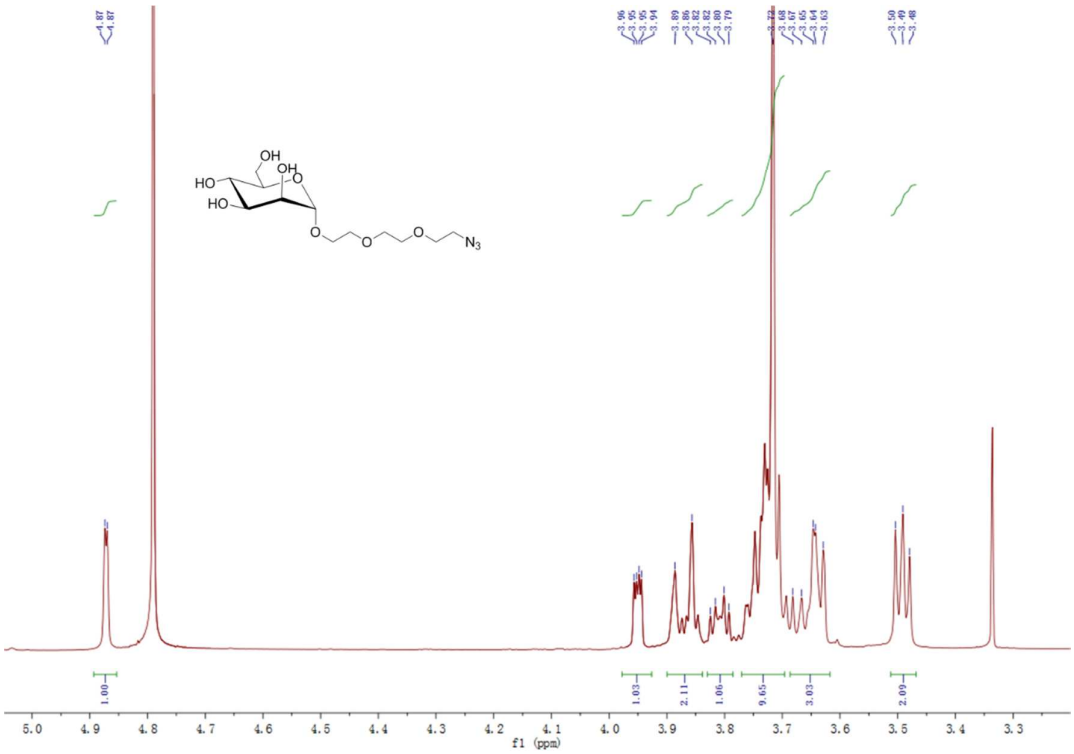

Figure S11. ^{1}H NMR spectrum (400 MHz, D_2O) of compound **4**.

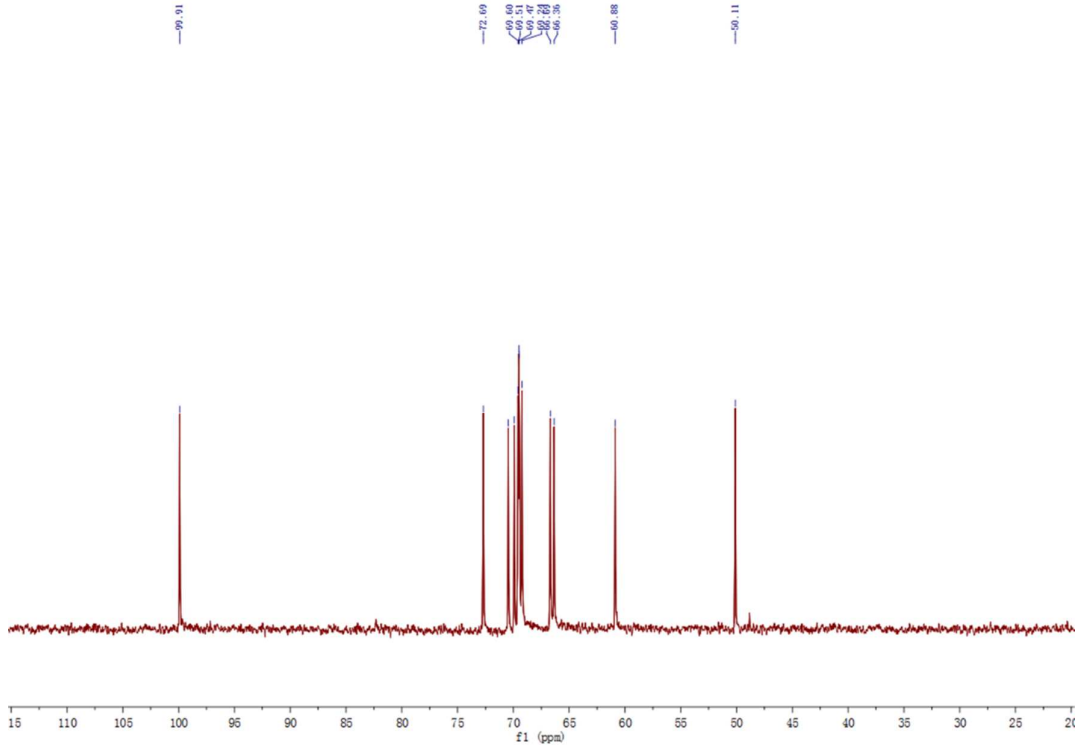

Figure S12. ^{13}C NMR spectrum (101 MHz, D_2O) of compound **4**.

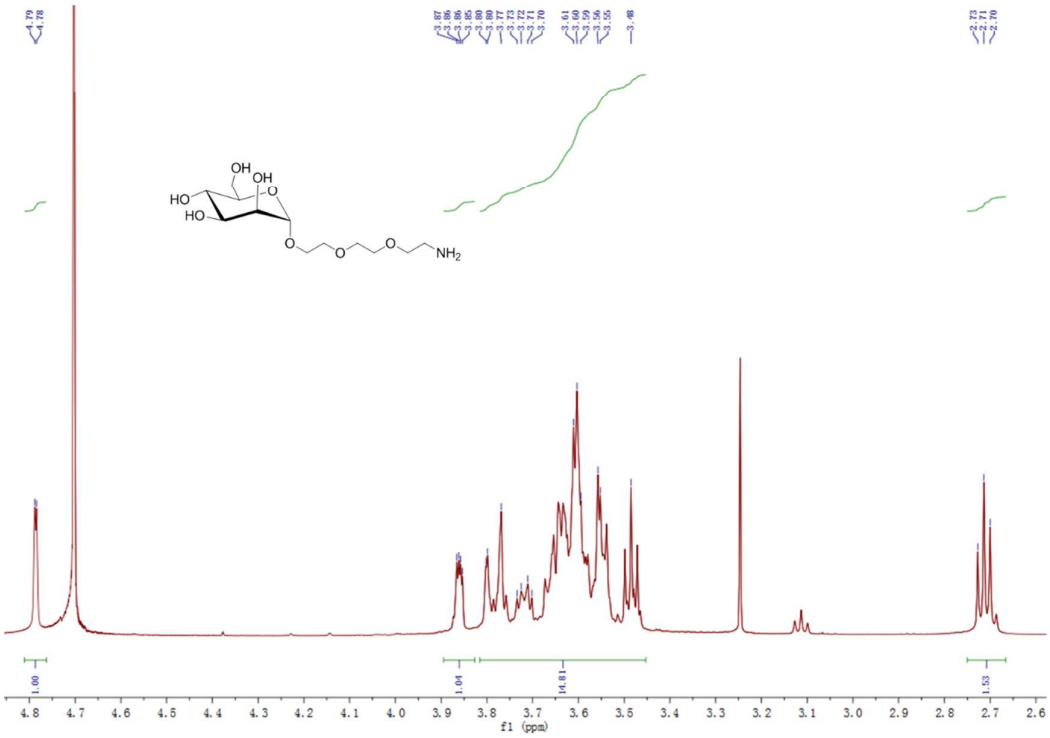

Figure S13. ^{1}H NMR spectrum (400 MHz, D_2O) of compound **5**.

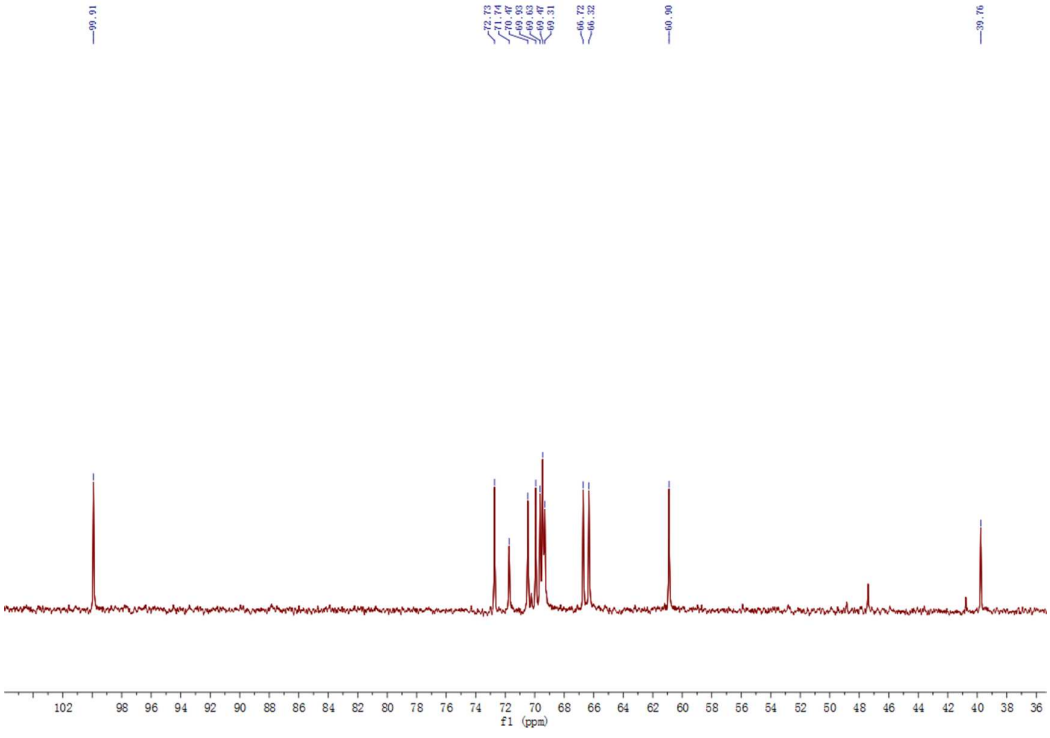

Figure S14. ^{13}C NMR spectrum (101 MHz, D_2O) of compound **5**.

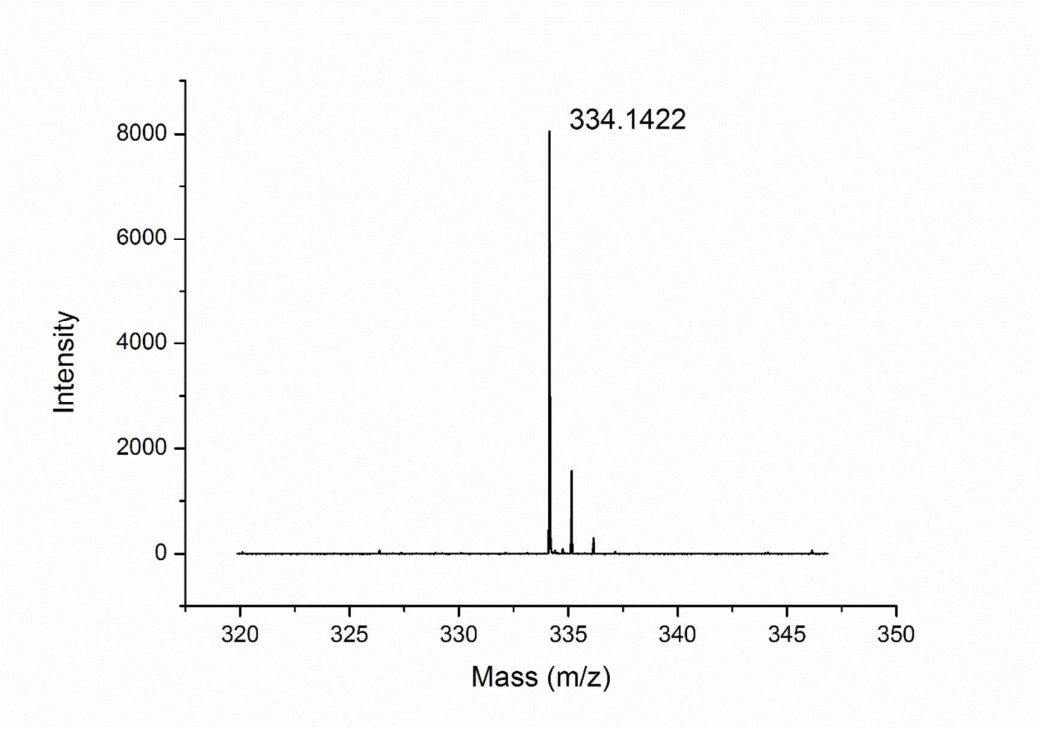

Figure S15. MALDI-TOF MS spectrum of compound **5**.

Crystallization-driven Self-assembly of PLLA-*b*-PTHPA to Prepare Cylindrical micelles 2 and 3 with Varied Lengths

In order to obtain cylindrical naonoparticles with different lengths, PLLA-*b*-PTHPA diblock was exposed to varied ratios of THF/H_2O.[5, 6] For shorter cylindrical micelles **2**, 0.125 mL of THF and 2.375 mL of water (resistivity 18.2 MΩ•cm) (v_{THF}/v_{H2O} = 5/95) were utilized while for longer cylinders **3**, 0.5 mL of THF and 2 mL of water (resistivity 18.2 MΩ•cm) (v_{THF}/v_{H2O} = 20/80) was used instead. The co-solvent was added to 50 mg of polymer inside a vial and acetic acid (1 eq. to the DP of PTHPA) was also added to the mixture to facilitate the hydrolysis of the THPA blocks. The vial was sealed

with a needle inserted through the seal and the mixture was allowed to stir at 65 °C during the evaporation of THF. After 30 h, the solution was quenched by cooling in liquid nitrogen and lyophilized. The freeze-dried PLLA-*b*-PAA nanoparticles **2** and **3** were then dissolved directly into water (0.25 mg/mL) for TEM and DLS analysis.

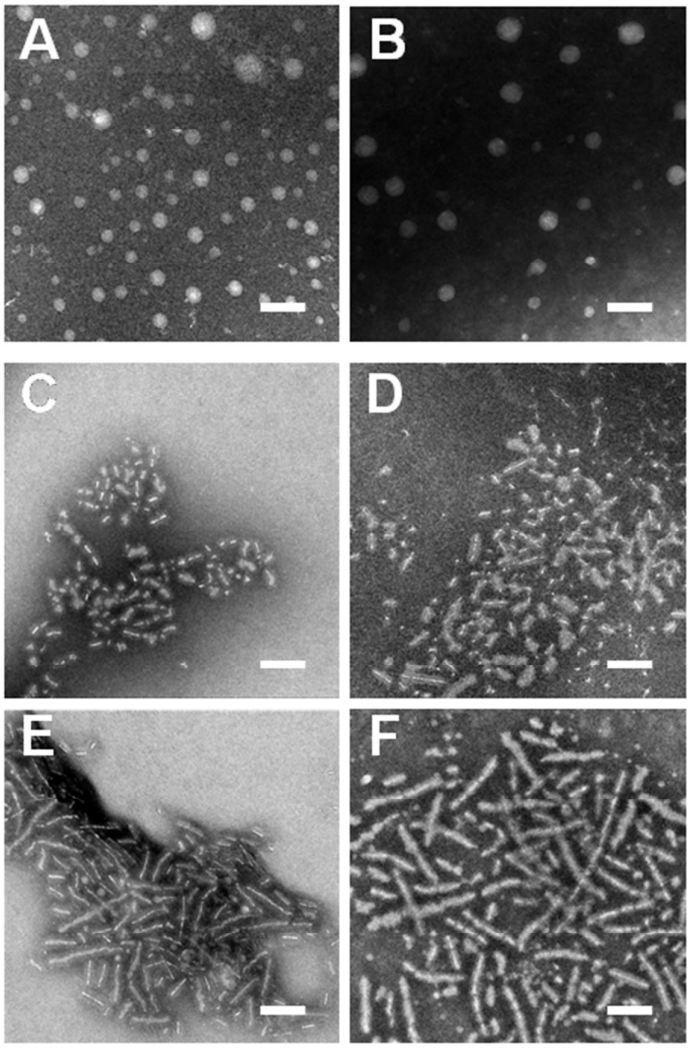

Figure S16. TEM images showing various nanoparticles before (A, C, E) and after (B, D, F) shell functionalizations with mannose. A

and B: spherical micelles **1** and **M1**; C and D: short cylindrical micelles **2** and **M2**; E and F: long cylindrical micelles **3** and **M3**. TEM samples were air-dried on carbon grids and were negatively stained using phosphotungstic acid (PTA). Scale bar = 200 nm.

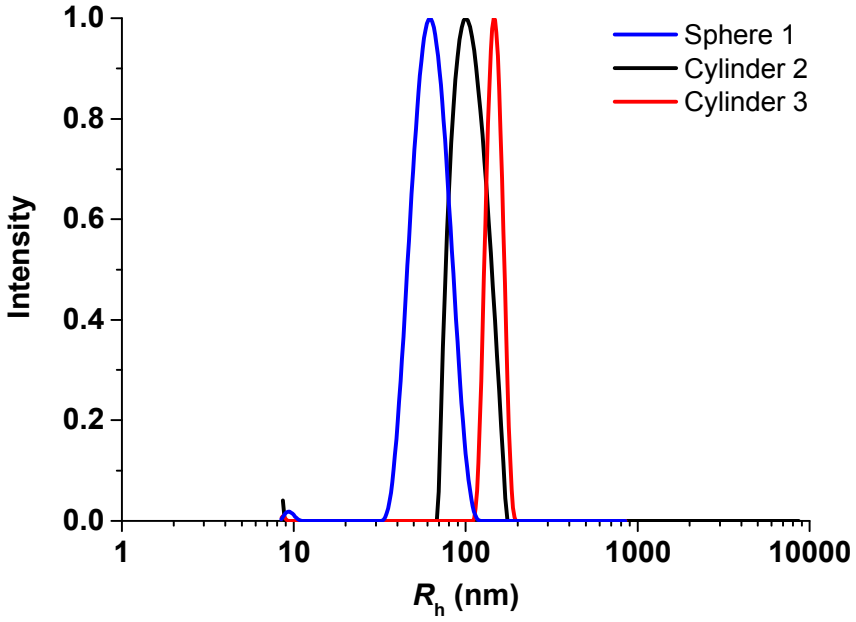

Figure S17. DLS data showing different R_h values of spherical micelles **1,** cylindrical micelles **2** and **3**.

Self-assembly of PDLLA-*b*-PTHPA to Prepare Spherical Micelles 1

Generally, 1 mL of THF and 1.5 mL of water (resistivity 18.2 MΩ•cm) (v_{THF}/v_{H2O} = 40/60) were added to 50 mg of polymer inside a vial. Acetic acid (1 eq. to the DP of PTHPA) was also added to the

mixture to facilitate the hydrolysis of the THPA blocks. The mixture was well-sealed and was allowed to stir at 65 °C for 30 h before being quenched by cooling in liquid nitrogen. The solution was then dialyzed against H_2O and lyophilized. The freeze-dried PDLLA-*b*-PAA spherical micelle **1** was then dissolved directly into water (0.25 mg/mL) for TEM and DLS analysis.

Shell Functionalization of Various Nanoparticles with Mannose and 5-Aminofluorescein (5-AF)

The amidation reactions were carried out using similar conditions as reported by Wooley and co-workers.[7] Typically, the freeze-dried cylindrical or spherical micelles were fully dissolved in H_2O (resistivity 18.2 MΩ•cm) (8 mg, 1 mg/mL). Then *N*-hydroxysulfosuccinimide (sulfo-NHS) (0.06 *eq.* to PAA) was added into the solution and was allowed to stir at 4 °C for 0.5 h. 1-Ethyl-3-(3-dimethylaminopropyl)carbodiimide hydrochloride (EDC•HCl) (0.45 *eq.* to PAA) was then added into the solution and was allowed to stir at 4 °C for 3.5 h. The pH of the solution was adjusted to *ca*. 7.0 using phosphate buffer (pH = 9.5, 0.1 M) before addition of 5-aminofluorescein (0.03 *eq.* to PAA dissolved in 1 mL DMSO). The amidation reaction was allowed to stir at 4 °C for 3 h and another 12 h at room temperature. Then a further sulfo-NHS (2

eq. to PAA) was added into the solution and was allowed to stir at 4 °C for 0.5 h. EDC HCl (1.5 *eq.* to PAA) was added into the solution and was allowed to stir at 4 °C for 4 h. The pH of the solution was adjusted to *ca*. 7.0 again using phosphate buffer (pH = 9.5, 0.1 M) before addition of amine functionalized mannose (1.5 eq. to PAA). The amidation reaction was allowed to stir at 4 °C for 3 h and another 27 h at room temperature before dialysis against deionized water for 2 days and subsequent lypholization to yield fluorescent spherical micelles **MF1,** cylindrical micelles **MF2** and **MF3**. To confirm the functionalization ratio, the freeze dried nanoparticles were dissolved in D_2O and were analyzed using ^1H NMR spectroscopy (400 MHz).

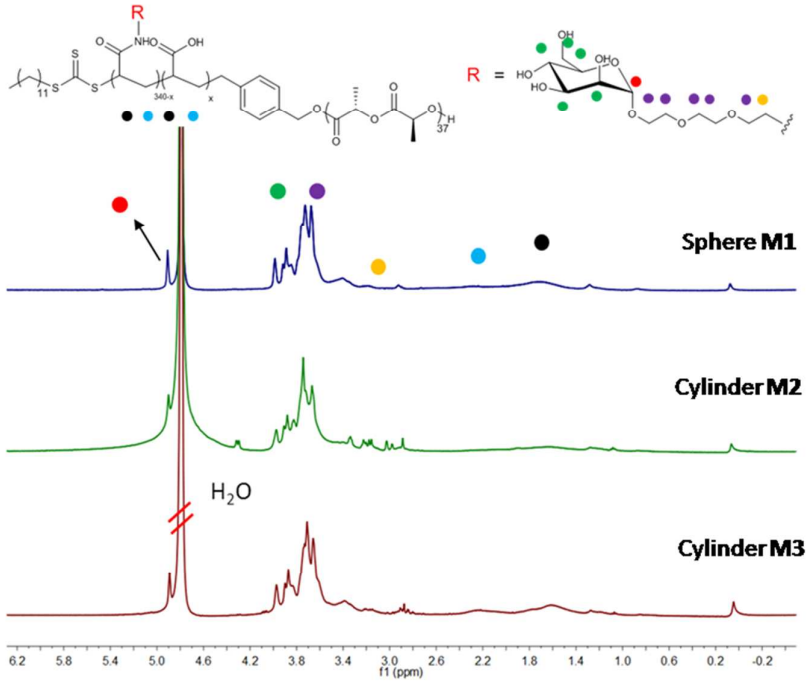

Figure S18. ^1H NMR spectrum (400 MHz, D_2O) of mannose

functionalized spherical micelles **M1**, cylindrical micelles **M2** and **M3**.

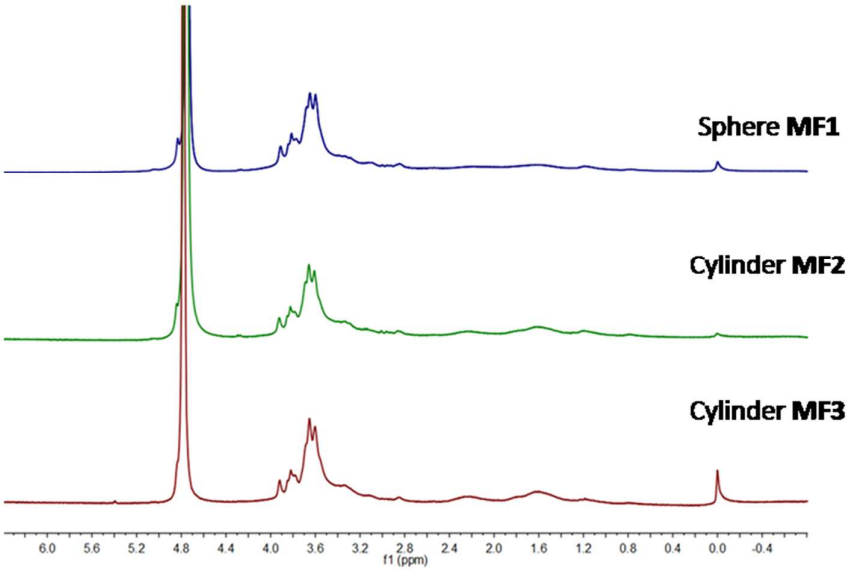

Figure S19. ^{1}H NMR spectrum (400 MHz, D_2O) of mannose and 5-AF functionalized spherical micelles **MF1,** cylindrical micelles **MF2** and **MF3**.

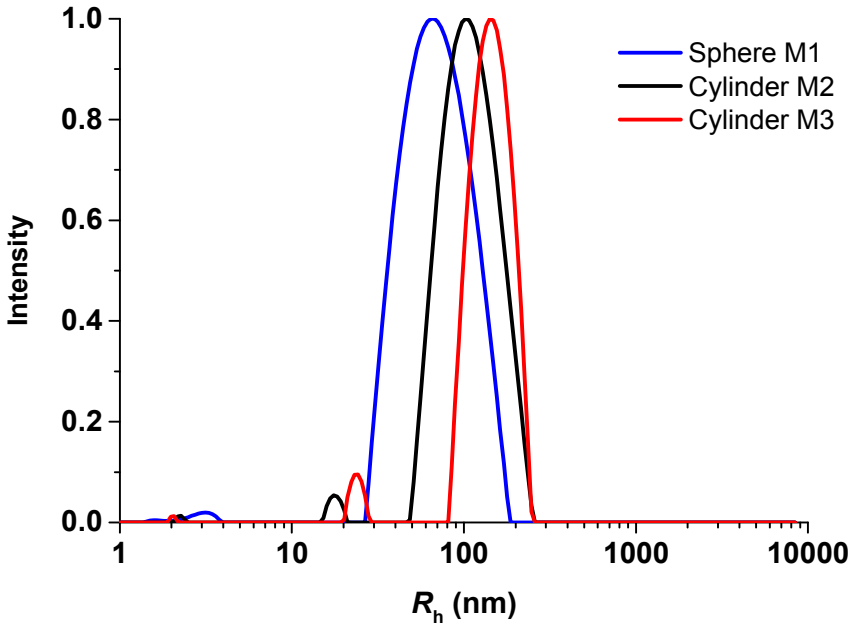

Figure S20. DLS data showing different R_h values of mannose functionalized spherical micelles **M1,** cylindrical micelles **M2** and **M3**.

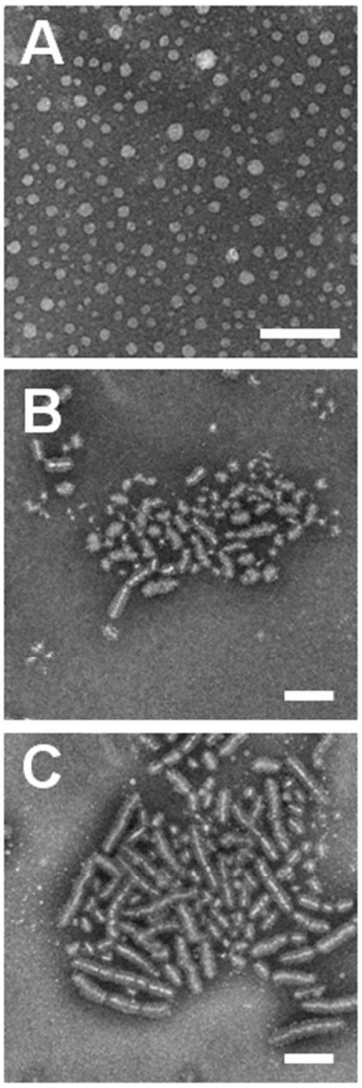

Figure S21. TEM images showing mannose and 5-AF functionalized spherical micelles **MF1** (A), cylindrical micelles **MF2** (B) and **MF3** (C).TEM samples were air-dried on carbon grids and were negatively stained using PTA. Scale bar = 200 nm.

Table S2. Characterization data of mannose and 5-AF functionalized spherical micelles **MF1,** cylindrical micelles **MF2** and **MF3**

Nanoparticle	L_n[a] (nm)	L_w/L_n	D_n[a] (nm)
Sphere **MF1**	—	—	33
Cylinder **MF2**	96	1.12	50
Cylinder **MF3**	203	1.18	53

[a] Measured by TEM analysis on stained samples (Figure S21).

Agglutination Test

Agglutination of GNPs and lectins was monitored in 1.00 mL semi-micro quartz cell at 25 °C at λ = 450 nm using UV-vis spectrometry. 80 μL of GNPs solution (0.125 mg/mL) was added into 500 μL of 50 mM lectin solution (the molar ratio of carbohydrate molecules to Con A is nearly 1:1). The mixture was shaken for 2 s before recording the absorbance change in time. All experiments were carried out in 20 mM HEPES buffer containing 300 mM NaCl, 5.0 mM $CaCl_2$ and 5.0 mM $MnCl_2$.

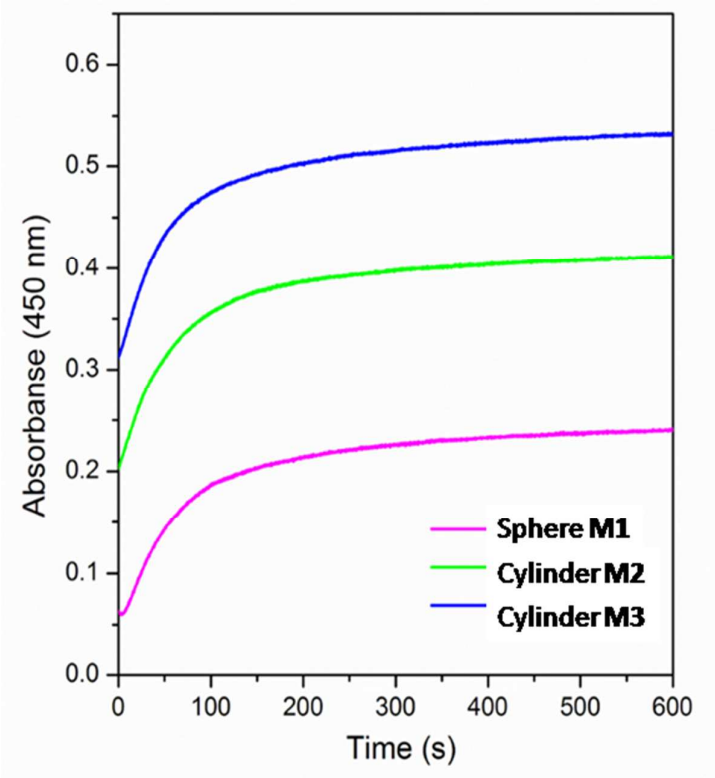

Figure S22. Agglutination assay of different GNPs with Con A in PBS buffer.

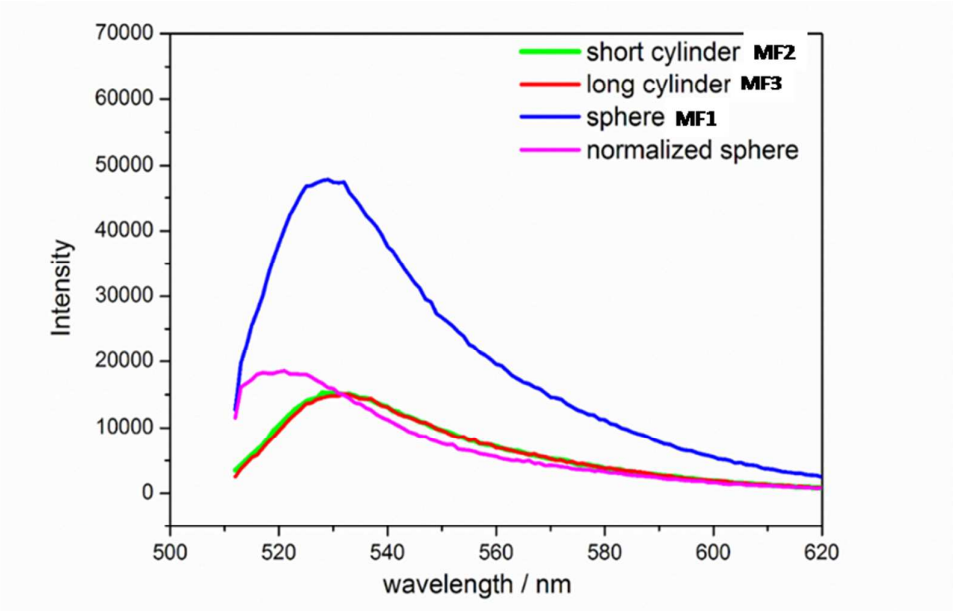

Figure S23. Fluorescent spectrum of various GNPs. Fluorescent spherical GNPs (**MF1**) were mixed with non-flurorescent spherical GNPs (**M1**) to reach similar fluorescence intensities of fluorescent cylindrical GNPs **MF2** and **MF3**.

Cytotoxicity evaluation of GNPs using cell counting kit-8 (CCK-8) assay

RAW264.7 macrophage cell line was cultured in a complete culture RPMI 1640 medium, supplemented with 10% fetal bovine serum (GIBCO) and 1% antibiotic antimycotic solution (GIBCO) at 37 °C and 5% CO_2 condition. In the cell viability experiments, RAW264.7 cells were cultured in 96 wells plate overnight, then different GNPs were added into culture medium at varied concentrations for 24 h.

Cell viability in response to GNPs was analyzed by CCK-8 assay (Dojindo) following the manufacturer's procedures. Generally, cell supernatant was removed and was washed with PBS for three times. CCK-8 reagent was added into wells in a ratio of 1/10 in culture medium. Cells were cultured in an incubator for 1 to 4 h. Finally, the plate was read with Microplate Reader (BioTex ELx800) in 450 nm.

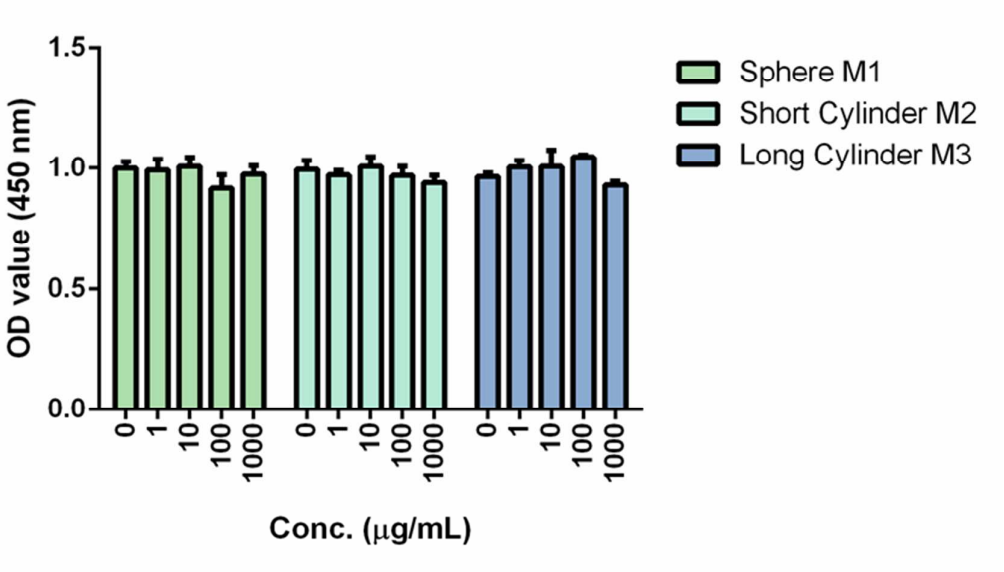

Figure S24. Cytotoxicity of GNPs determined by CCK-8 assays.

Cellular uptake of GNPs

RAW 264.7 cells were seeded on 24 wells plate at a concentration of 10^5/mL overnight. Then cells were treated with fluorescent GNPs **MF1**, **MF2** or **MF3** at different concentration (0 to 100 μg/mL in culture medium) for 4 h or with different incubation time (0 to 24 h) at a concentration of 10 μg/mL. Cells were washed with PBS buffer

for three times to remove non-binding GNPs and collected for endocytosis analysis on flow cytometer (Beckman Gallios). Endocytosis was represented by the mean of fluorescent intensity. Statistic data were presented as means ± SEM. Data were analyzed with one-way ANOVA. The statistical significance level was set as $*p < 0.05$ and $**p < 0.01$.

Confocal laser scanning microscopy

RAW264.7 macrophages were seeded on glass bottom cell culture dishes (2×10^5 cells/dish) using a complete culture RPMI 1640 medium, supplemented with 10% fetal bovine serum (GIBCO) and 1% antibiotic antimycotic solution (GIBCO). Cells were cultured overnight before the addition of GNPs. After incubation for 4 h, the culture medium was removed and the cells were washed three times with PBS. The cells were fixed with 4% formaldehyde for 10 min and washed with PBS for three times. The nuclei were stained with DAPI (3 μm) for 5 min and washed with PBS for three times. Fluorescence images of cells were obtained using confocal microscopy (Nikon C2+).

Endocytosis inhibition study

RAW264.7 cells were seeded on 24 wells plate at a concentration of 10^5/mL overnight. Cells were treated with different inhibitors of endocytosis pathways for 2 h followed by the addition of fluorescent GNPs and left for another 4 h. Chloropromazine (20 μg/mL) was used to inhibit clathrin-mediated endocytosis, genistein (200 μM) was used to inhibit caveolae-mediated endocytosis while rottlerin (10 μM) was used to block macropinocytosis. Then the cells were washed with PBS buffer for three times and were collected for flow cytometry analysis. Endocytosis was represented by the mean of fluorescent intensity. Statistic data were presented as means ± SEM. Data were analyzed with one-way ANOVA. The statistical significance level was set as $*p < 0.05$ and $**p < 0.01$.

Cytokine Assay

RAW264.7 cells were seeded in 24 well plate at a concentration of 10^5/mL overnight. Then the cells were treated with GNPs (10 μg/mL in culture medium) for 24 h. Supernatant was collected and centrifuged to remove GNPs and dead cells. Cell supernatant was then detected with ELISA for cytokine secretion following the manufacturer's procedures. Generally, capture antibody was coated in 96-well plate overnight. Wells were blocked with BSA

buffer. Then standard or samples were added to the appropriate wells at room temperature and left for 2 h, followed by the addition of detection antibody and avidin-HRP. TMB was added for color development. The optic densities at 450 nm were determined using a Microplate Reader (BioTek ELx800) within the linear regression. Each sample was measured in triplicates. Data were presented as means ± SEM. Data were analyzed with one-way ANOVA. The statistical significance level was set as *$p < 0.05$ and **$p < 0.01$.

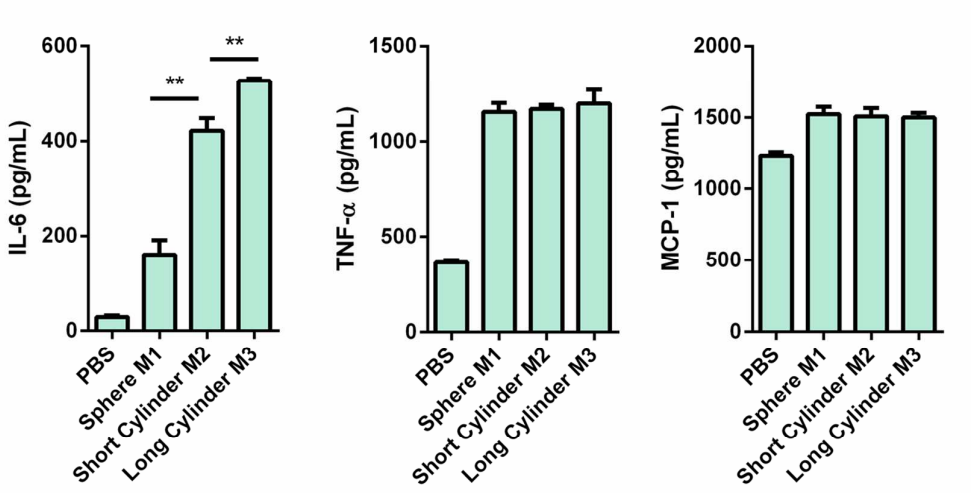

Figure S25. GNPs (2 μg/mL for spherical GNPs, 10 μg/mL for short cylindrical GNPs and long cylindrical GNPs) promoted the (A) IL-6, (B) TNF-α, (C) MCP-1 secretion of macrophages after 24h incubation measured by ELISA. Data are expressed as the mean ± SD of three independent experiments. * $p < 0.05$ and ** $p < 0.01$.

References

1. Pratt, R. C.; Lohmeijer, B. G. G.; Long, D. A.; Lundberg, P. N. P.; Dove, A. P.; Li, H. B.; Wade, C. G.; Waymouth, R. M.; Hedrick, J. L. *Macromolecules* **2006,** 39, (23), 7863-7871.

2. Hertler, W. R. *US Patent* **1991,** No. 5 072 029.

3. O'Reilly, R. K.; Joralemon, M. J.; Hawker, C. J.; Wooley, K. L. *Chem. Eur. J.* **2006,** 12, (26), 6776-6786.

4. Petzetakis, N.; Dove, A. P.; O'Reilly, R. K. *Chem. Sci.* **2011,** 2, (5), 955-960.

5. Sun, L.; Petzetakis, N.; Pitto-Barry, A.; Schiller, T. L.; Kirby, N.; Keddie, D. J.; Boyd, B. J.; O'Reilly, R. K.; Dove, A. P. *Macromolecules* **2013,** 46, (22), 9074-9082.

6. Petzetakis, N.; Walker, D.; Dove, A. P.; O'Reilly, R. K. *Soft Matter* **2012,** 8, (28), 3408-3414.

7. Xu, J. Q.; Sun, G. R.; Rossin, R.; Hagooly, A.; Li, Z. C.; Fukukawa, K.; Messmore, B. W.; Moore, D. A.; Welch, M. J.; Hawker, C. J.; Wooley, K. L. *Macromolecules* **2007,** 40, (9), 2971-2973.